Automatic Detection of Bone Contours in X-Ray Images

Alexey Mikhaylichenko[1], Yana Demyanenko[1], and Elena Grushko[2]

[1] Institute of Mathematics, Mechanics and Computer Science,
Southern Federal University, Rostov-on-Don, Russia,
{alexey.a.mikh,demyanam}@gmail.com,
[2] Southern Federal University, Rostov-on-Don, Russia,
elena.i.grushko@gmail.com

Abstract. Detection of bone contours in x-ray images is an important step in the computer analysis of medical images. Analog X-ray images are characterized by low contrast ratio value and high variability of their optical properties. Therefore classical segmentation algorithms based on homogeneity criteria are not applicable. In this paper we propose an approach for automatic bone contours detection which does not require homogeneity of regions. This method is based on accurate edge fragments detection and elimination of discontinuities between them. We have defined the criteria for calculating numerical characteristics of the quality of image contours detection. The obtained results are used for diagnosis of abnormalities and diseases of the detected object.

Keywords: X-ray bone segmentation, Medical x-ray images, Contour extraction, Registration, Image processing, Object detection.

1 Introduction

Digital images are currently widely applied for disease diagnostics in medical science. Using Roentgen radiation for radiograph (X-ray image) acquisition, which allows detecting fractures, bone abnormalities and other diseases, is one of the most widely-spread and cost effective non-invasive medical monitoring methods. However, most of the papers on medical images segmentation are focused on CT- and MRI images. In this paper we present the method developed for X-ray images analysis.

We concentrate on the problem of automatic segmentation of bone structures in X-ray images. Low contrast ratio value of the analog X-ray images along with their optical properties complexity is one of the major challenges in solving this problem. In particular, objects in the radiography images have irregular texture and intensity. Consequently, traditional segmentation techniques based on thresholding, region growing, clustering, watershed transformation etc. cannot be applied, since their implementation requires exact regions homogeneity test. Deformable models (snakes, active contour models) can be used for X-ray image segmentation, but an accurate initial estimate is necessary to this end, otherwise the segmentation result can be unacceptable.

In this paper we propose an approach for automatic bone contours detection which does not require homogeneity of regions. It can be used for joint recognition in X-ray images. This method is based on accurate edge fragments detection and elimination of discontinuities between them. We have defined the criteria for calculating numerical characteristics of the quality of image contours detection. The obtained results can be applicable for diagnosis of abnormalities and diseases of the detected object.

2 Overview

As discussed in Section 1, classical segmentation algorithms based on homogeneity criteria are not applicable. In paper [1] the authors propose to eliminate the weakness of homogeneity criteria by means of interaction with the user. At first mean-shift algorithm is used for initial segmentation. The initial segmentation produces a set of small regions. After that a region merging algorithm is used. Region merging technique is based on the markers placed by the user. The method gives very accurate results. However, the proposed segmentation method is interactive and it requires user interactions. This restricts its applicability.

Some techniques of contours extraction are based on using 2D template of the desired object or some other a priori knowledge about it [2,3,4,5]. First, the initial position of template on the image is identified. Then the method of active contours with the initial template is used for the identified region [6]. The important problem for such methods is the search for the accurate initial position on an image. The result of applying the method of active contours in many ways depends on it (Fig. 1, a). Generalized Hough transform is frequently used for searching the initial position. In paper [2] an incremental approach to segmentation of femur bones is proposed. The salient features in x-ray images, including parallel lines, circles etc are used for searching the initial position.

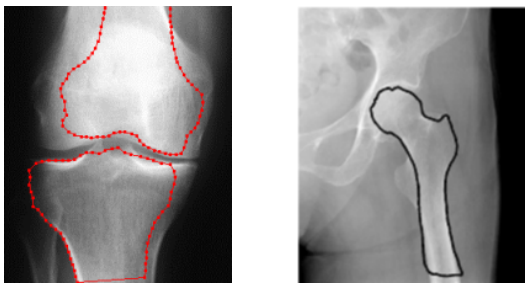

a) b)

Fig. 1. Typical problems of methods, which use template. (a) Incorrect identification of initial position [5]; (b) one of the candidate solution is acceptable but not ranked at the top [2]

However, the methods which use templates have significant limitations. They are not applicable for detecting objects with strong shape distortion. And in cases of medical images such objects are of particular interest. In the article [2] the authors demonstrate an example of an incorrect contours extraction in cases of fractured femur with severe shape distortion and healthy bones with fuzzy shape (Fig. 1, b).

The paper [3] solves a similar problem (femur segmentation). The proposed algorithm is based on active shape model. The major contribution is that a regularization term representing the smoothness of shape change in each iteration is incorporated. This reduces limitations of methods, which use templates.

We propose an approach which does not use a priori information about the shape of the object. This allows us to avoid problems arising from the strong distortion of the shape.

3 Contour detection method

Let I be an input X-ray image (Fig. 2, a), i.e.

$$I = \{I(x, y) \in [0, 255] \,|\, 1 < x \leq M, 1 < y \leq N\}\,.$$

Before starting the image undergoes light blurring to eliminate spot noise. The best results were obtained using bilateral filtration algorithm [7]. As a preliminary, a binary version of input image I^{bin} is computed with a threshold evaluated with Otsu's method [8]. In order to get a more consistent and integral result, morphological dilation with small disk radius can be applied to I^{bin}.

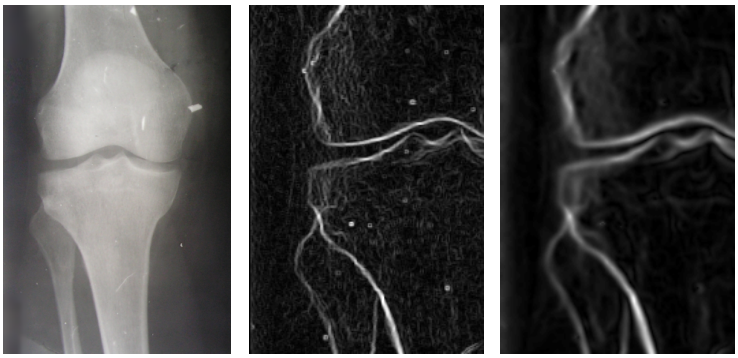

a) b) c)

Fig. 2. (a) Original image; (b) Kirsch operator applied to original image; (c) gradient vector flow field (GVF)

At this stage the image gradient ∇I is computed, for the purpose we suggest Kirsch operator [9] (Fig. 2, b). Let $|\nabla I|$ and I^{dir} denote gradient magnitude and

gradient direction respectively. Furthermore, the gradient vector flow (GVF) is calculated (Fig. 2, c). Although Kirsch or Sobel operator detects edges correctly, its scope is limited: fairly large gradient values are obtained only in immediate proximity to the edge, whereas the values for other regions are close to zero. GVF doesn't have this limitation. Detailed description and groundings of GVF computing methods are available in [10].

We further proceed with an image, which is element-wise multiplication of gradient magnitude and GVF magnitude, we denote it by G_1 (Fig. 3, a). For this image, an estimated binarization threshold T^* is computed. Edge thinning operation is then conducted by using GVF direction values. We denote the resulting image by G_2 (Fig. 3, b).

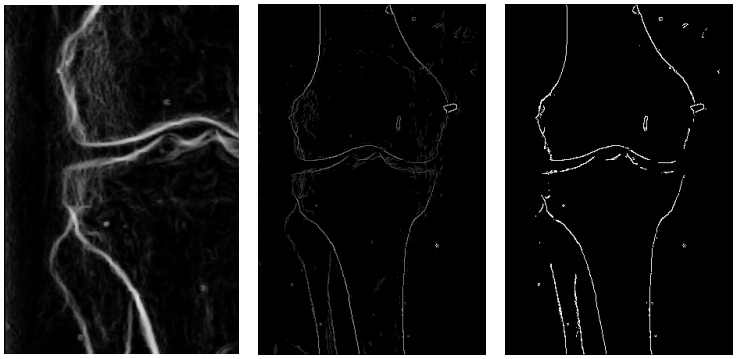

a) b) c)

Fig. 3. Result of element-wise multiplication $G_1 = |\mathbf{v}| * |\nabla I|$; (b) G_2 — result of applying non-maximum suppression to G_1; (c) result of binarizing G_2 with optimal threshold

The next stage is finding binarization threshold for the image G_2. We find it in αT^* form, where α denotes a coefficient in the range $(0, 1]$. For all α involved, binarization threshold of the image G_2 with αT^* is conducted. The obtained binary image contains fragments of the object boundaries. For merging these fragments into contours special algorithms have been devised. After finishing the discontinuities elimination procedure we get an image with the target contours. The quality of obtained contours detection is then numerically estimated, as defined within the research. After computing the estimates for various threshold values it remains to choose α value such that the estimate is the best, we denote it by α^*. Further processing involves contours obtained with binarization threshold $\alpha^* T^*$.

The resulting contours are refined with active contour method [6]. It is worth noting that before applying the method we should ensure that the traversal ordering for all contours will be the same. The equality of contour ordering is also important on the recognition stage. Subsequently, it becomes possible to

classify the objects whose contours were detected (e.g. bone type definition, getting its healthy/normal condition or defects detection).

3.1 Pre-processing

Let $\mathbf{v} = [u(x,y), v(x,y)]$ denote gradient vector flow field of input image. $\mathbf{v}^{dir}$ and $|\mathbf{v}|$ are computed using the formulas:

$$|\mathbf{v}| = \sqrt{u^2 + v^2},\ \mathbf{v}^{dir} = \arctan\frac{v}{u}.$$

Let G_1 denote the result of element-wise multiplication $|\mathbf{v}|$ and $|\nabla I|$:

$$G_1 = |\mathbf{v}| * |\nabla I|.$$

Direction values $\mathbf{v}^{dir}$ are rounded off to the nearest 45°, following 8-adjacency of a pixel. The image G_1 then undergoes non-maximum suppression using $\mathbf{v}^{dir}$. The operation is similar to edge thinning in Canny edge detection algorithm [11]. The resulting image is G_2.

3.2 Binarization threshold T^* evaluation

For computing the threshold T^* we use the image G_1. The algorithm includes 2 steps:

1. Brightness gradient magnitude is calculated for each pixel of the image

   $$\widehat{G}(x,y) = \max(|G_{1,x}(x,y)|, |G_{1,y}(x,y)|).$$

   Directional derivatives $G_{1,x}$, $G_{1,y}$ are regarded as discrete analogs of differentiation operator:

   $$G_{1,x}(x,y) = G_1(x+1,y) - G_1(x-1,y),$$
   $$G_{1,y}(x,y) = G_1(x,y+1) - G_1(x,y-1).$$

2. Target threshold is calculated according to formula

   $$T^* = \frac{\sum_{y=1}^{N}\sum_{x=1}^{M} G_1(x,y)\cdot\widehat{G}(x,y)}{\sum_{y=1}^{N}\sum_{x=1}^{M}\widehat{G}(x,y)}. \quad (1)$$

3.3 Chaining

Let G^{bin} denote an image obtained by binarizing G_2 with some threshold. This image contains fragments of edges. We propose an approach of chaining the fragments, i.e. elimination of discontinuities between the fragments that belong to one contour. Chaining algorithm includes two stages. At the first stage, we eliminate discontinuities for pairs of pixels. At the second stage, we process pixels left unpaired. Both stages run iteratively. At each iteration we remove discontinuities whose length is less than a defined constraint K. We increase K at each iteration.

Discontinuity points

Let $U(p)$ denote a set of pixels of a boundary which are adjacent to p (i.e. pixels for which $G^{bin}(p_i) = 1$), $|U(p)|$ denotes cardinality. Pixels of the boundary are assumed 8-adjacent: $|U(p)| \leq 8$, ρ denotes Euclidean distance between the points. We distinguish 3 types of discontinuities in boundaries (Fig. 4):

1. a point, for which $|U(p)| \leq 1$
2. a point, for which
$$U(p) = \{p_1, p_2\} :$$
$$\rho(p_1, p_2) = 1,\ x_1 = x_2 \vee y_1 = y_2$$
3. a point, for which
$$U(p) = \{p_1, p_2, p_3\} :$$
$$\rho(p_1, p_2) = 1,\ \rho(p_1, p_3) = 1,\ x_1 = x_2,\ y_1 = y_3$$

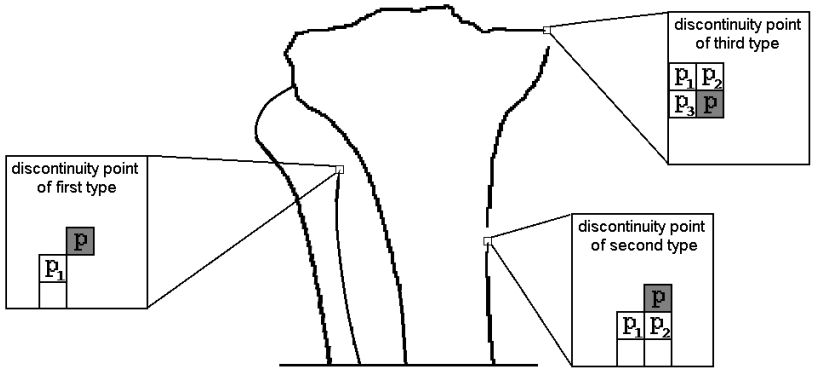

Fig. 4. Types of discontinuity points

The first stage

Let p and q denote discontinuity points, r — a point adjacent to p. We define $\overline{u}$ as a vector codirectional with r-to-p vector. Coefficient d denotes deviation range between points q and p in the $\overline{u}$ direction (see Fig. 5).

Knowing $\overline{u}$ direction and d value, we define vectors $\overline{v}$ and $\overline{\omega}$ to limit area of searching the discontinuity point associated with p point:

$$v_x = u_x \cos(-d) - u_y \sin(-d),$$
$$v_y = u_x \sin(-d) + u_y \cos(-d),$$
$$\omega_y = u_x \cos d - u_y \sin d,$$

$$\omega_y = u_x \sin d + u_y \cos d.$$

If q is located between limiting vectors $\overline{v}$ and $\overline{\omega}$ with origin p (2), then we attempt to eliminate discontinuity between p and q.

$$\omega_x t_y - \omega_y t_x \geq 0,\ t_x v_y - t_y v_x < 0, \tag{2}$$

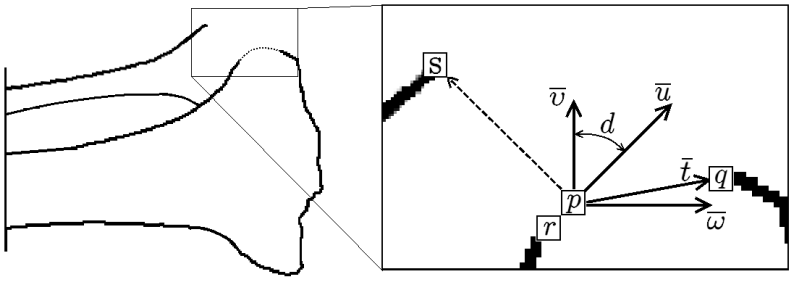

Fig. 5. Condition of discontinuity existence between p and q. In this case the condition holds: q is located between $\overline{v}$ and $\overline{\omega}$. S is out of scope

Chaining implies finding a set of 8-adjacent pixels that provide 8-adjacency of p and q, i.e. finding a path between p and q.

For path search we apply algorithm A^*, which is an extension of Dijkstra's algorithm demonstrating acceptable results on a plain grid. We apply following heuristics:

- the entire image is traversable;
- the cost of point p traversal is $|\nabla I(p)|$ value multiplied by -1;
- the cost of point-to-point transfer includes Euclidian distance and absolute difference of gradient values;
- the next point selection relies on heuristic evaluation of distance to the target.

The range of $|\nabla I|$ values is preliminary scaled. The larger the gradient values range, the more precise obtained curve retraces the boundary of the target object. Some regions of the image contain densely spaced bounds of two different objects. In that case the algorithm can jump to another object's bound due to gradient identity. Therefore it's important to fit the scaling coefficients. In this paper we suggest mapping $|\nabla I|$ values to $[0, 10]$.

Let us denote found path by $\Gamma = \{\gamma_i\}_{i=1}^{L}$, average gradient value of the entire image by ξ, path cost by Φ:

$$\xi = \frac{1}{NM} \sum_{x=1}^{M} \sum_{y=1}^{N} |\nabla I(x, y)|,$$

$$\Phi = \sum_{i=1}^{L} |\nabla I(\gamma_i)|.$$

For the found path, we check 2 conditions:

1. Path cost is more than conditional cost $\Phi' = L \cdot \xi \cdot \theta$:
$$\Phi > \Phi'. \tag{3}$$
Parameter θ is directly-proportional to restriction K on length of the discontinuity being removed;
2. Γ does not intersect already existing fragments of bounds on the image G^{bin} (Fig. 6, left);

If the conditions hold, we assert that points of Γ belong to target bounds on the image G^{bin} (Fig. 6, right).

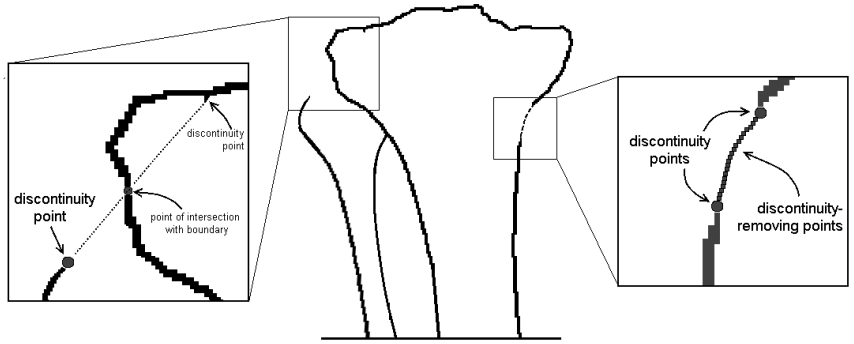

Fig. 6. Violation of the second condition (left) and example of the removing a discontinuity (right)

The second stage

For an unpaired point of discontinuity, the curve Γ is grown following the gradient. Next point of the curve is chosen in a direction orthogonal to gradient in the previous point. We halt growing the curve if we reach a pixel for which at least one of the following conditions holds:

1. it is an element of some bound fragment (Fig. 7, left):
$$(x, y): \quad G^{bin}(x, y) = 1; \tag{4}$$
2. it is a border pixel of the image (Fig. 7, right):
$$(x, y): \quad x \in \{1, M\} \vee y \in \{1, N\}. \tag{5}$$

We do not consider the curves whose length exceeds the constraint K. If condition (3) holds for Γ, then we assert that points of Γ belong to target bounds on the image G^{bin}.

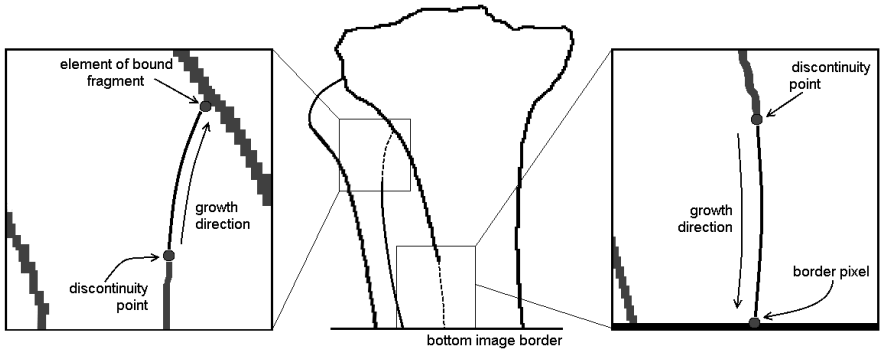

Fig. 7. Chaining on condition 4 (left) and chaining on condition 5 (right)

3.4 Numerical estimate of edge detection quality

Let W denote a set of image I pixels whose intensity values exceed binarization threshold found by applying Otsu's algorithm to I.

We further denote bounded region by Ω, number of the region pixels by $|\Omega|$, W cardinality within Ω region by $w(\Omega)$, average pixels intensity value of image I in region Ω by $avg(\Omega)$, number of binary image A pixels whose intensity value exceeds binarization threshold by $v(A)$:

$$w(\Omega) = \sum_{p \in \Omega} I^{bin}(p),$$

$$avg(\Omega) = \frac{1}{|\Omega|} \sum_{p \in \Omega} I(p),$$

$$v(A) = \sum_{p \in S} A(p),\ S = [1, M] \times [1, N].$$

Our prime interest is in the regions Ω_i such that:

1. $avg(\Omega_i)$ exceeds the threshold found by applying Otsu's method to image I;
2. $|w(\Omega_i) - |\Omega|| < \varepsilon$.

We denote class of such regions by $\overline{\Omega} = \bigcup_{i=1}^{n} \Omega_i$. We estimate edge detection quality with

$$E = \frac{w(\overline{\Omega})}{v(I^{bin})} \left(1 - \frac{v(\overline{G} * I^{bin})}{v(I^{bin})}\right) \left(1 - \frac{|\overline{\Omega}| - w(\overline{\Omega})}{NM - v(I^{bin})}\right), \tag{6}$$

where $\overline{G}$ denotes binary image after applying chaining algorithm.

3.5 Threshold computation

We adjust threshold for the best contour detection. To that end, we use suggested numerical estimate. We propose an algorithm of threshold computation in the form αT^* as follows.

For all α in $(0, 1]$ with some increment, we execute the following steps:

1. binarizing image G_2 with threshold αT^*;
2. obtained binary image undergoes chaining procedure, the resulting image is $\overline{G}$;
3. edges of the objects are extracted on the image $\overline{G}$;
4. obtained set of contours is numerically estimated by E_α.

After computing E_α we search α^*:

$$\alpha^* = \underset{\alpha}{\operatorname{argmax}} E_\alpha.$$

The result of final edge detection is a set of contours detected with threshold $\alpha^* T^*$.

To refine the detected edges, active contour method can be applied. The suggested detection method assures that small iterations number of active contour method is required.

4 Experimental results

We tested the algorithm for X-ray images of knee and elbow joint in lateral and coronal view, with various resolution, quality and distortion of bones. We have tested about 100 X-ray images provided by Rostov State Medical University.

The efficiency evaluation results of the proposed method are presented in Table 1. Contours on 74% of test images were successfully extracted, despite the variations in shapes, sizes and shape distortion of the bones (Fig. 8). $14,2\%$ of the images are marked as a partial success (Fig. 9, a, b). The other $11,8\%$ do not have acceptable results (Fig. 9, c). Failed samples contain such artifacts as noise or many false borders, caused by the process of obtaining analogue images.

Table 1. Efficiency of proposed method

Result	Part of all test images
Successful detection	74%
Partial success (false border detection)	$14,2\%$
Incorrect detection	$11,8\%$

The processing time the test images for computer 2.4GHz Core i7 is presented in Table 2.

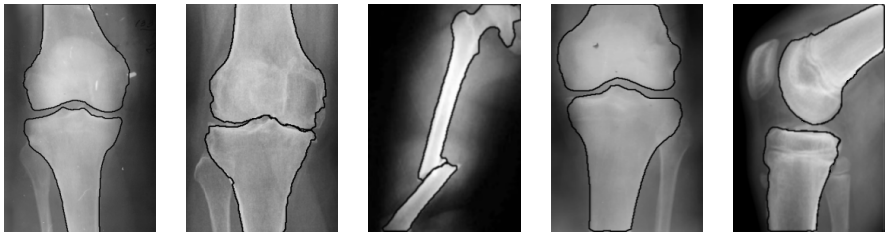

a) b) c) d) e)

Fig. 8. Sample of test results. Despite variations in shapes, sizes and shape distortion of bones in images, correct contours are extracted

a) b) c)

Fig. 9. The sample of unsuccessful applications of the method: detection of false boundaries (a), (b) and over-segmentation (c)

Table 2. Evaluation of time complexity of proposed method for specific images

Image	Resolution	Time complexity (s)	
		single-threaded	multi-threaded
Fig. 8, a	292×450	$0,92$	0.55
Fig. 8, b	226×450	$2,5$	1.74
Fig. 8, c	201×294	$0,612$	0.418
Fig. 8, d	231×365	$0,462$	0.409
Fig. 8, e	240×344	$1,096$	0.7
Fig. 9, a	250×450	$1,6$	0.82
Fig. 9, b	300×442	$2,65$	1.506
Fig. 9, c	258×406	$3,3$	2.13

5 Conclusion

The paper introduces the method of automatic detection of bone contours in medical X-ray images. It is based on boundary fragments detection with further chaining them to contours. The method does not require homogeneity, the lack of which is typical for X-ray images. Numerical estimate of edge detection quality is also proposed.

Algorithm specificity provides an opportunity to make good use of parallelizing the computation (in particular on the stages of chaining and threshold adjusting). This implies high-speed performance of the developed program.

The method was tested on a set of medical images provided by Rostov State Medical University.

In contrast to methods based on template matching, the suggested approach is applicable for detecting the objects of badly distorted shape (bone fractures, flail joint etc). Consequently, it is suitable not only for health status evaluation but for classifying defects in joints within health screening as well.

References

1. Stolojescu-Crisan, C., Holban, S.: An Interactive X-Ray Image Segmentation Technique for Bone Extraction. International Work-Conference on Bioinformatics and Biomedical Engineering, pp. 1164–1171 (2014).
2. Chen, Y., Ee, X. H., Leow, W. K., Howe, T. S.: Automatic Extraction of Femur Contours from Hip X-ray Images. Computer Vision for Biomedical Image Applications, pp. 200–209 (2005)
3. Behiels, G., Vandermeulen, D., Maes, F., Suetens, P., and Dewaele, P.: Active shape model-based segmentation of digital x-ray images. Proceedings of the Second International Conference on Medical Image Computing and Computer-Assisted Intervention, pp. 128–137 (1999)
4. Garcia, R. L., Fernandez, M. M., Ignacio Arribas, J. I., Lopez, C. A.: A fully automatic algorithm for contour detection of bones in hand radiographs using active contours. IEEE International Conference on Image Processing, pp. 421–424 (2003)
5. Chernuhin, N. A.: On an approach to object recognition in X-ray medical images and interactive diagnostics process. IEEE Proceedings: Computer Science and Information Technologies (CSIT) (2013)
6. Williams D. J., Shah M.: A Fast Algorithm for Active Contours and Curvature Estimation. CVGIP: Image Processing. Volume55, No 1, January. – P. 14–26 (1992)
7. Tomasi C., Manduchi R.: Bilateral filtering for gray and color images. Sixth International Conference on Computer Vision. IEEE, pp. 839—846 (1998)
8. Otsu, N.: A threshold selection method from gray-level histograms. IEEE Trans. Sys., Man., Cyber. 9: 62–66 (1979)
9. Kirsch R.: Computer determination of the constituent structure of biological images. Computers and Biomedical Research, 4. – P. 315—328, (1971)
10. Xu C., Prince J. L.: Snakes, Shapes, and Gradient Vector Flow. IEEE Transactions on Image Processing, 7(3), pp. 359–369, (1998)
11. Canny, J.: A Computational Approach To Edge Detection. IEEE Trans. Pattern Analysis and Machine Intelligence, 8(6):679-–698 (1986)